Contact Space Analysis for Narrow-Clearance Assemblies [1]

Gordon Dakin Robin Popplestone

CS Technical Report 93-59

July 9, 1993

Abstract

A technique is described for modelling the 6–dimensional contact space of an assembly with narrow insertion clearances. A nominal assembly mating trajectory is supplied a priori *by a high-level planner, using assembly part models with zero clearance at the sites of insertion. Augmented with small, user-specified clearances, the local contact space surrounding any "problematic" configuration in the nominal trajectory is analyzed and represented as an adjacency graph of contact states. The contact states represent the zero- to five-dimensional facets of contact space. The facets' nonlinear surface representations permit a more exact characterization of contact space topology than described previously [7]. The vertices of a local contact space are calculated by intersecting 6–tuples of primitive contact surfaces via the multivariable Newton method, whose rapid convergence to vertex configurations provides an efficient means of analyzing local contact space topologies. Subtuples of the vertices' primitive contacts give rise to the adjacent, higher-dimensional facets of contact space, forming an adjacency graph of contact states. As described in a companion paper [6], a heuristic search of the adjacency graph yields a traversable sequence of contact states.*

[1]Preparation of this paper was supported by grant IRI-9208920 and CDA-8922572 from the National Science Foundation.

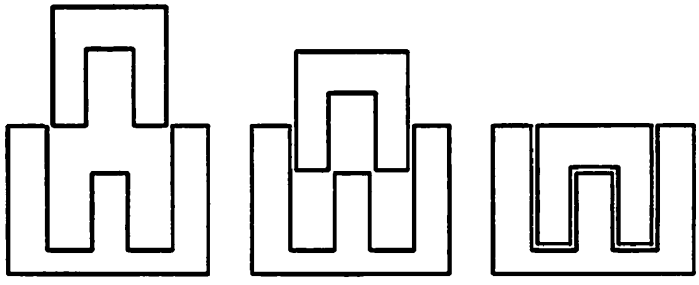

Figure 1. The critical points in a nominal trajectory.

1 Introduction

Fine-motion planning for assembly is concerned with the planning of jam-free sliding motions to achieve a goal configuration or a set of spatial relationships between the assembly parts. A fine-motion plan must accommodate the uncertainty arising from limited precision in position sensing, robot control, and the assembly part models. In the *two-phase approach* to planning with uncertainty, a nominal motion plan is first derived from kinematic constraints alone, and then modified to address the effects of sensing, control, and model error. Together with a companion paper [6], the present paper is concerned with the latter phase of the two-phase approach, in which a fine-motion planner automatically synthesizes sliding trajectories within the local contact spaces surrounding problematic configurations in the original nominal trajectory. Here we address the representation of a local contact space, to support the formation of fine-motion trajectories described in [6].

The two-phase approach to fine-motion planning differs fundamentally from the *LMT methods* [9][16], which synthesize multistep, nominal trajectories in a "single phase", through the recursive backchaining of subgoal regions. The LMT approach is both more rigorous and more complete than the "two-phase" approach, whose reliance on an initial plan formed without uncertainty considerations may restrict the set of fine-motion plans it can generate. On the other hand, the LMT methods fail to utilize "obvious" geometric information that can simplify the planning process, such as the symmetries of the assembly

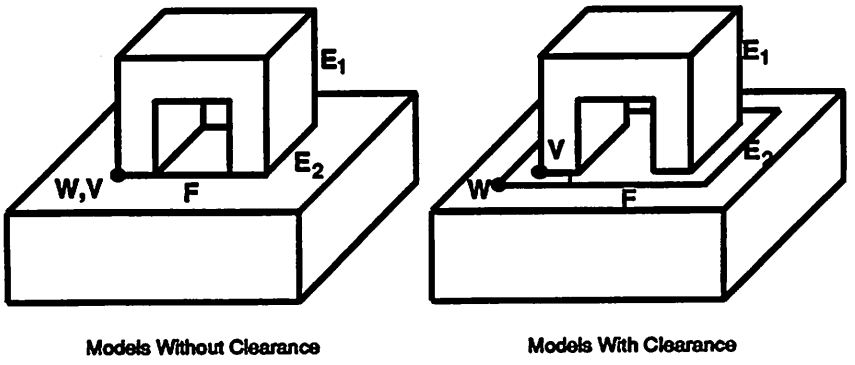

Figure 2. Introducing clearances to the part models.

parts. Moreover, the double-exponential complexity of the LMT approach [5] has prevented its implementation outside of very restrictive domains.

In the current approach, a high-level assembly planner [15] first derives a nominal trajectory from geometric constraints alone, using solid models whose dimensions do not yet allow for clearances at the insertion sites. The *critical points* in the nominal trajectory are then identified (see figure 1), indicating the configurations where jamming and collisions are likely to occur. Narrow insertion clearances are then introduced to the assembly part models, as specified by the designer of the parts (see figure 2). The small clearances give rise to a local, 6-dimensional contact space around each critical point configuration. To support the search for an appropriate sequence of contact state transitions to safely maneuver the assembly past the problematic critical points, an adjacency graph of contact states is constructed for each local contact space. The analysis and construction of a local contact space is the subject of the present paper. As described in [6], a heuristic search of the resulting contact state graph yields a deterministic sequence of contact events involving the formation or separation of one contact at a time.

1.1 Relationship to other methods

Although our fine-motion planning technique falls into the "two-phase" category of fine-motion planning methods, it differs from methods in which uncertainty is accommodated in the second phase by way of *corrective compliance* [17][19][20]. In that approach, a single control strategy is designed to correct

deviations of the moving part from the nominal path, which is retained as the command trajectory. The present approach *replaces* the nominal trajectory with fine motions planned within the local contact spaces surrounding the critical points in the original trajectory.

The method currently employed to construct a local contact space is related to that of Koutsou [13], who identified the vertices of global contact space by enumerating 6-tuples of spatial relationships, which were combined algebraically, using an extension of RAPT [18]. Our technique, however, invokes the multivariable Newton method to solve for the vertex configurations. The restriction of the assembly motion to a determinate sequence of states (as we describe in [6]) was essential to the methods of Caine and his colleagues [3][4], who wished to simplify the *manual* task of designing a force control strategy that would satisfy each state's jamming constraints. Our technique relies on heuristics to select an appropriate sequence of contact states, whereas Donald [8], Laugier [14], and the authors [7] previously employed heuristics in the formation of curvilinear trajectories. Finally, our iterative calculation of piecewise-linear trajectory segments [6] is related to the *flexible trajectory* techniques of gross motion planning [2][10], whereby an arbitrary trajectory is first hypothesized, and then optimized through a gradient descent procedure.

2 Primitive Contacts

The introduction of clearances to the assembly part models gives rise to 6 degrees of freedom in the pose of the moving part relative to the stationary part. Within each local C-space, the moving part's pose is characterized as a point vector $\mathbf{X}$ in $\Re^6$, consisting of a translational perturbation $\mathbf{dx} = [dx\ dy\ dz]^T$ and a rotational perturbation $\delta\mathbf{x} = [\delta x\ \delta y\ \delta z]^T$ of the moving part away from the C-space origin (the critical point configuration). The translational component $\mathbf{dx}$ represents the homogeneous transformation

$$trans(dx, dy, dz) = \begin{pmatrix} 1 & 0 & 0 & dx \\ 0 & 1 & 0 & dy \\ 0 & 0 & 1 & dz \\ 0 & 0 & 0 & 1 \end{pmatrix} \tag{1}$$

and the rotational component $\delta\mathbf{x}$ denotes *roll-pitch-yaw* angles of successive

rotations about the z, y, and x axes [2]:

$$RPY(\delta x, \delta y, \delta z) = rotz(\delta z)\, roty(\delta y)\, rotx(\delta x) \tag{2}$$

$$= \begin{pmatrix} C_z & -S_z & 0 & 0 \\ S_z & C_z & 0 & 0 \\ 0 & 0 & 1 & 0 \\ 0 & 0 & 0 & 1 \end{pmatrix} \begin{pmatrix} C_y & 0 & S_y & 0 \\ 0 & 1 & 0 & 0 \\ -S_y & 0 & C_y & 0 \\ 0 & 0 & 0 & 1 \end{pmatrix} \begin{pmatrix} 1 & 0 & 0 & 0 \\ 0 & C_x & -S_x & 0 \\ 0 & S_x & C_x & 0 \\ 0 & 0 & 0 & 1 \end{pmatrix}$$

where the S_i and C_i denote the sine and cosine of δx_i.

The local 6-dimensional configuration space surrounding a critical point is bounded by 5-dimensional C-surfaces, which correspond to the *primitive contacts* (PCs) that can occur near the critical point. For polyhedral objects, each PC is a single-point contact involving either a convex vertex and a face, or two convex edges. As shown in figure 2, the PCs that can occur in the presence of insertion clearances are just the PCs that occur simultaneously between the two parts prior to introducing clearances to their models. Moving part vertex V, for example, lies on the border of stationary part face F in the clearance-free assembly, indicating the presence of the corresponding C-surfaces in the contact space of the models that include clearances. The existence of a primitive contact between edges E_1 and E_2 is similarly inferred by noting that their line segments meet in the clearance-free models.

The C-surface of primitive contact PC_i is characterized by a function $f_i : \Re^6 \rightarrow \Re$. A moving part pose $\mathbf{X}$ lies on the C-surface of PC_i if $f_i(\mathbf{X}) = 0$. Each C-surface function f_i is derived from the geometries of the assembly part features involved, and the clearance between the two features. The geometry of a vertex-face contact is illustrated in figure 3. Vector $\mathbf{r}$ represents the position of vertex V relative to the moving part origin $\mathbf{p}$, and clearance vector $\mathbf{dc}$ represents the separation between the vertex and face G when the moving part is positioned at the critical point. The geometries of face-vertex and edge-edge contacts are shown in figures 4 and 5, respectively.

The C-surface equation of a PC is derived by asserting that a point on the moving part feature and a point on the stationary part feature share the same ordinate along the PC's *contact normal* $\mathbf{n}_c$:

$$(\mathbf{p} + \mathbf{dx} + RPY(\delta\mathbf{x})\,\mathbf{r}) \cdot \mathbf{n}_c = (\mathbf{p} + \mathbf{r} + \mathbf{dc}) \cdot \mathbf{n}_c \tag{3}$$

[2]The reverse order of rotations stems from the use of global, as opposed to successively rotated, rotational axes.

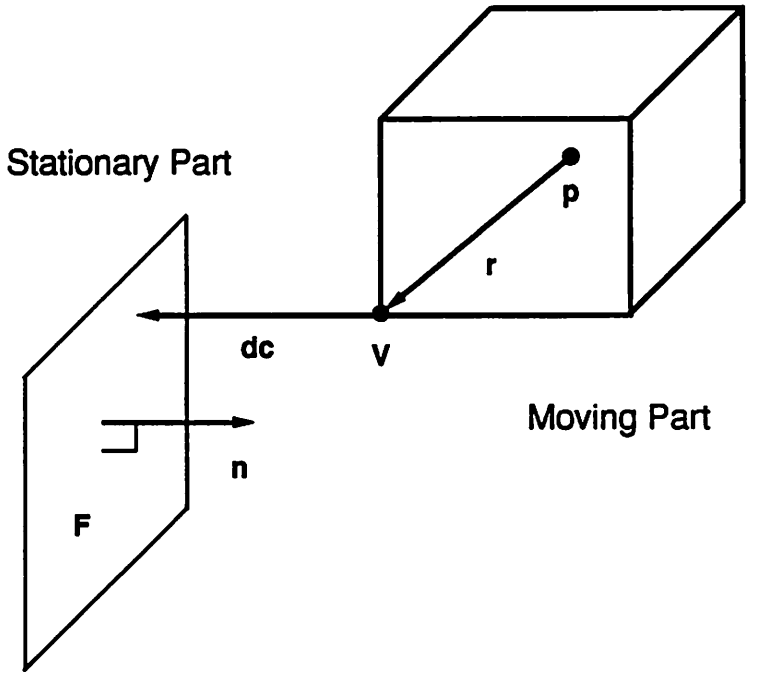

Figure 3. A vertex-face contact.

For vertex-face contacts, $\mathbf{n}_c$ is just the outward normal $\mathbf{n}$ of the stationary face. For face-vertex contacts, $\mathbf{n}_c = -RPY(\delta\mathbf{x})\ \mathbf{n}$, while for edge-edge contacts, $\mathbf{n}_c$ is parallel to $\pm RPY(\delta\mathbf{x})\ \mathbf{v} \times \mathbf{w}$. Equation 3 yields a transcendental C-surface function $f_i(\mathbf{X})$, which is shown in Appendix I. The equation $f_i(\mathbf{X}) = 0$ describes a 5–dimensional C-surface that locally divides $\Re^6$ into halfspaces corresponding to "free space" and the *forbidden zone*, the subset of $\Re^6$ where the assembly parts overlap. Adopting the convention that $\mathbf{n}_c$ points away from the stationary part feature, the poses $\mathbf{X}$ on the "free space" side of the C-surface correspond to $f_i(\mathbf{X}) > 0$. The poses for which $f_i(\mathbf{X}) < 0$ lie on the side of the forbidden zone.

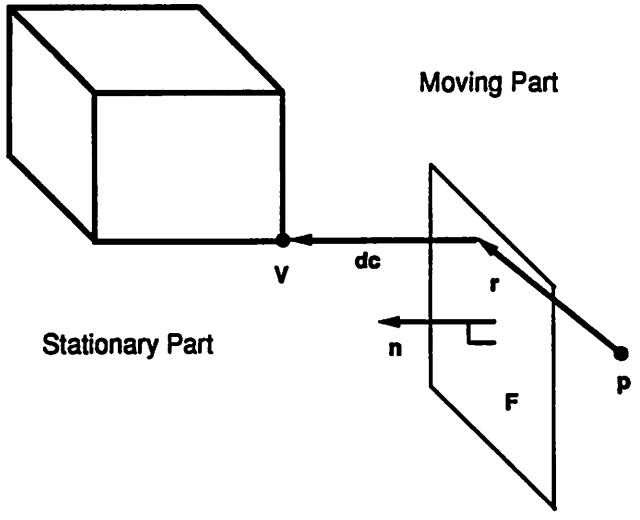

Figure 4. A face-vertex contact.

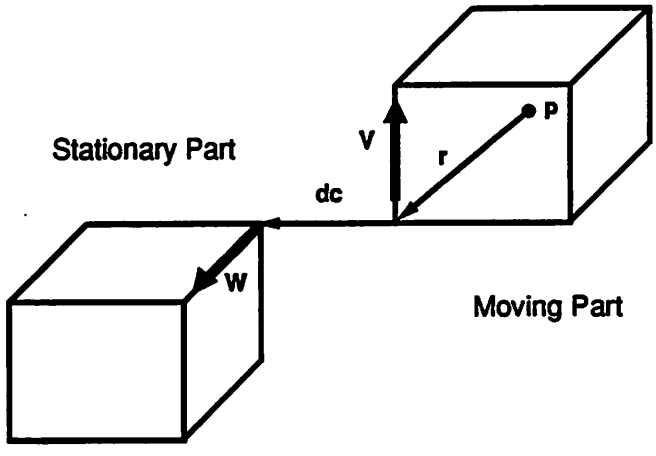

Figure 5. An edge-edge contact.

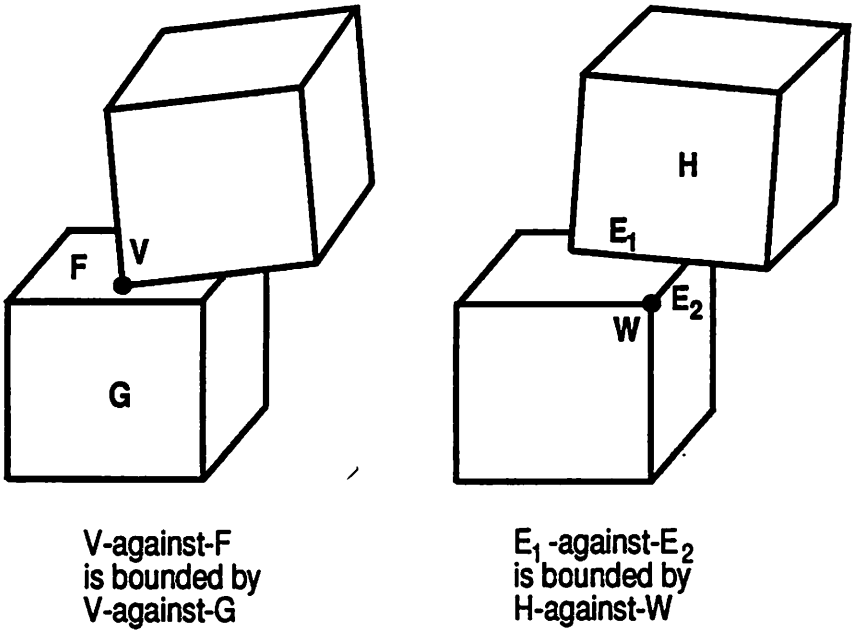

Figure 6. Primitive contact bounds.

The outward normal to PC_i's C-surface, $\mathbf{N}_i$, and a formula for the PC's hyperplanar tangent surface, are expressed in Appendix II as functions of the pose $\mathbf{X}$. In section 3, the tangent hyperplanes of 6 PC surfaces are intersected to yield a contact space vertex point in $\Re^6$.

The 5-dimensional contact space facet associated with a PC may have borders corresponding to the finite extent of the assembly part surface features, as well as borders arising from adjacent contacts. In figure 6, the contact involving vertex V and face F is bounded by the convex edge shared by F and its adjacent face G. The poses $\mathbf{X} \in \Re^6$ associated with the PC formed by V and F are confined to the halfspace $g(\mathbf{X}) < 0$, where g is just the C-surface function for the contact between V and G. The V-against-G contact is called a *bounding contact* of the V-against-F contact. In general, a primitive contact PC_i has some n_i bounding contacts PC_{ij}. Assuming the part faces of all vertex-face and face-vertex contacts are convex, the half-
spaces $g_j(\mathbf{X}) < 0$ of a PC's bounding contacts intersect to form a convex region in $\Re^6$. If a part face is concave, it is divided into convex faces prior to the enumeration of the PCs.

Each PC's facet in contact space, and the forbidden zone of overlapping configurations behind the facet, are represented by point sets expressed in terms of the C-surface functions $f_i(\mathbf{X})$. The *forbidden zone* F_i of PC_i is the region of $\Re^6$ behind PC_i's C-surface and its bounding contacts:

$$F_i = \{\mathbf{X} \in \Re^6 \mid f_i(\mathbf{X}) < 0,\ f_{ij}(\mathbf{X}) < 0, j = 1 \ldots n_i\} \tag{4}$$

The entire forbidden zone $\mathcal{F}$ surrounding a critical point's local C-space is formed by the union of all the PCs' forbidden zones:

$$\mathcal{F} = \cup_i F_i \tag{5}$$

The point set S_i in $\Re^6$ associated with a primitive contact PC_i consists of the portion of the contact's C-surface that lies behind its border PCs' C-surfaces but not in the forbidden zone:

$$S_i = \{\mathbf{X} \mid f_i(\mathbf{X}) = 0,\ f_{ij}(\mathbf{X}) < 0, j = 1 \ldots n_i, \mathbf{X} \notin \mathcal{F}\} \tag{6}$$

Expressions (4), (5), and (6) are easily implemented as predicates, using the C-surface functions $f_i(\mathbf{X})$ found in Appendix I. Expression (6) is utilized in section 3 to verify that a vertex formed by the interection of 6 PCs lies in each PC's point set, which excludes overlapping configurations.

Since the forbidden zone is generally concave, a PC_i's point set S_i is usually concave as well and cannot be represented by a single intersection of halfspaces. For the purpose of efficiently measuring the distance between a trajectory segment and a PC's point set [6], however, it is preferable to represent PCs as convex sets, even if they overlap the forbidden zone. When calculating distances between trajectory segments and "obstacle" PCs, a PC's closest point may then lie in the forbidden zone of a closer, intervening obstacle PC, but the closer PC's presence will overshadow the importance of the former obstacle PC.

Ignoring the presence of the forbidden zone, PC_i and its n_i bounding contacts PC_{ij} define a *convex* point set

$$S_i' = \{\mathbf{X} \mid f_i(\mathbf{X}) = 0,\ f_{ij}(\mathbf{X}) < 0, j = 1 \ldots n_i\} \tag{7}$$

whose polytopic approximation typically requires only two or three hyperplanar facets. As described in the companion paper [6], affine space representations of these facets are readily computed from the hyperplanar tangents of PC_i and its bounding contacts PC_{ij}, which are formulated in Appendix II.

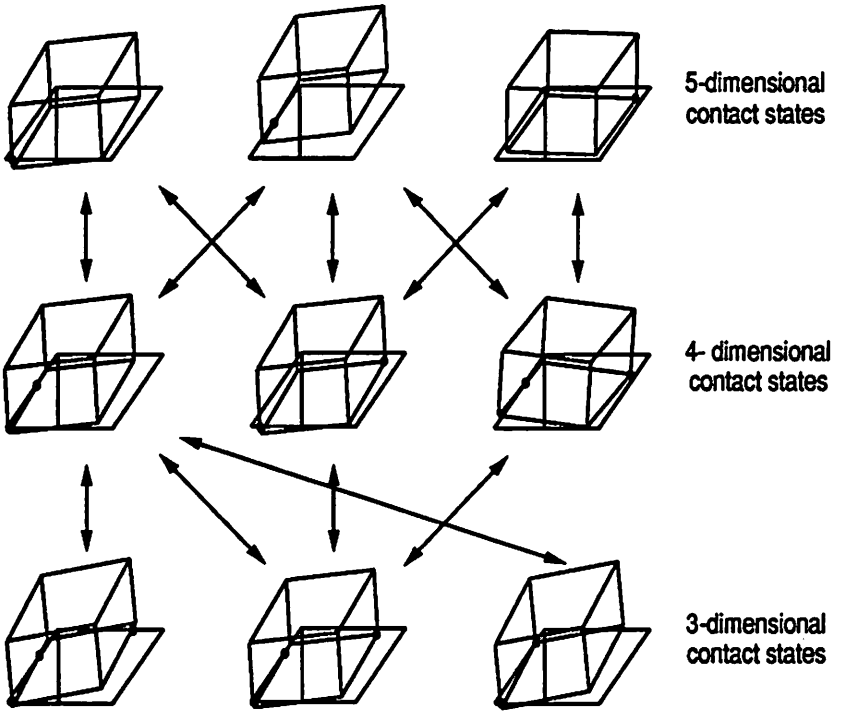

Figure 7. Adjacency graph of contact states.

3 Contact space topology

In this section, we describe the formation of an adjacency graph of contact states to represent the topology of local contact space. The contact state graph is constructed by a fine-motion planner to support the heuristic search for a sequence of contact state transitions [6]. Figure 7 illustrates a small portion of the adjacency graph for the square peg-in-hole assembly task.

The first step in constructing the local contact space surrounding a critical point is the enumeration of its vertices (0-dimensional facets). The vertices are obtained by computing all of the legal moving part configurations determined by 6-tuples of primitive contacts. This combinatorial method was employed by Koutsou [13], who combined the spatial relationships of 6 PCs symbolically to yield each vertex configuration. The current technique, however, obtains the vertex configurations numerically, via the multivariable Newton method.

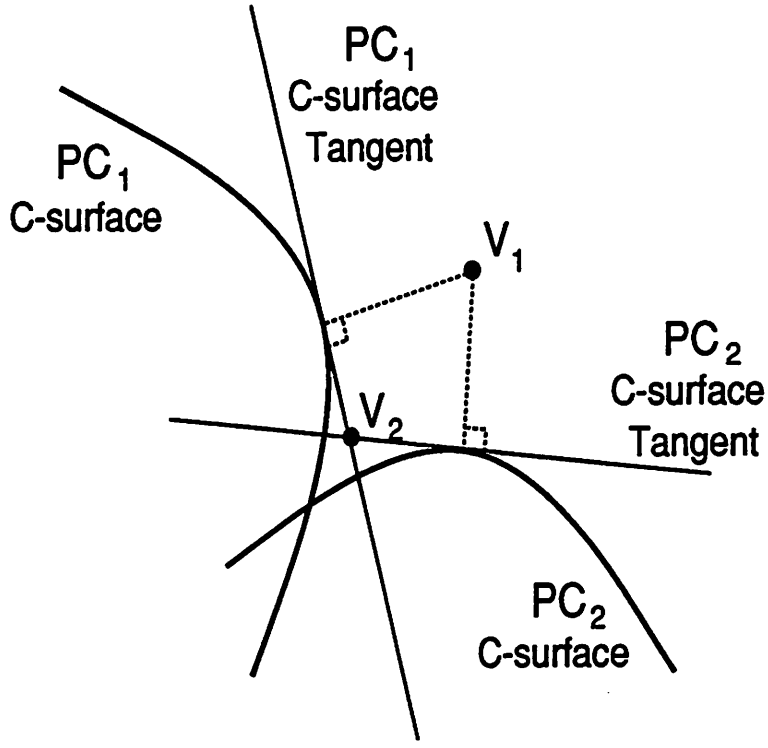

Figure 8. Vertex calculation through iterative refinement.

The point of intersection V associated with the C-surfaces of 6 primitive contacts $PC_1, \ldots, PC_6$ is just the common root of the C-surface equations $f_i(\mathbf{V}) = 0$, $i = 1..6$. Given an initial estimate of V, the multivariable Newton method iteratively refines the estimate, converging rapidly to its true position. For low-clearance assemblies, the vertices of contact space are never more than a perturbation away from the origin, so the origin itself provides a suitable first approximation.

As figure 8 shows in 2 dimensions, the initial estimate $\mathbf{V_1}$ of the vertex point where two C-surfaces intersect gives rise to two C-surface tangents, which intersect at an improved vertex estimate $\mathbf{V_2}$. An initial estimate (e.g., the origin) of the vertex is thus iteratively refined until its measurable modification ceases. For 3-dimensional assemblies, the C-surface tangent equation for each of six PC_is is obtained by parameterizing the tangent formula shown in Appendix

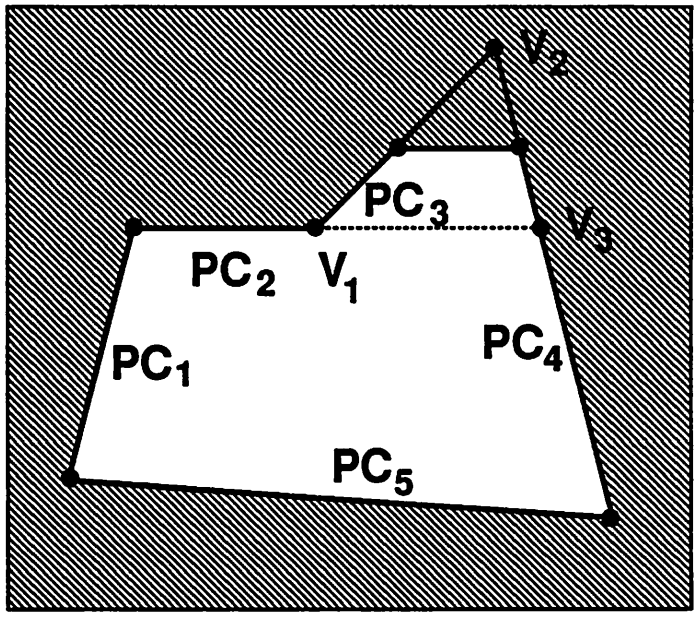

Figure 9. Identifying nonspurious contact space vertices.

II with the successively refined poses $\mathbf{V_i}$. Each refined vertex approximation $\mathbf{V_i}$ is then obtained by simultaneous solution of the 6 PCs' surface tangent equations, yielding the point in $\Re^6$ where the 6 C-surface tangents intersect.

If the C-surfaces of 6 primitive contacts $PC_1, \ldots, PC_6$ intersect at a single point $\mathbf{V}$ in $\Re^6$, then $\mathbf{V}$ corresponds to a contact space vertex iff it lies in the point set S_i of each of its associated PC_is. Computationally, this is verified by testing whether $\mathbf{V}$ satisfies the predicate associated with each PC's point set expression (6), which excludes the forbidden zone. Figure 9 shows the analogy in 2-dimensional contact space. Each candidate vertex is formed by intersecting the C-surfaces of a pair of PCs. V_1 is found to be a legitimate vertex, since it lies within the point sets of its constituent contacts PC_2 and PC_3. V_2, on the other hand, lies in the forbidden zone, and V_3 lies in the point set of only one of its PCs.

Once the vertices of a local contact space have been identified and located, the 1-dimensional edges of contact space are generated by enumerating the 5-tuples of PCs contained in the vertices' 6-tuples. The 4-tuples of the edges'

PCs give rise to the 2-dimensional facets of contact space, and so on. Each new and distinct contact state thus enumerated is placed in an adjacency graph (see figure 7), together with arcs denoting whether a contact state's set of PCs is a subset of an adjacent "son" state's set of PCs. Each arc in the graph denotes the establishment or separation of a single contact.

4 Implementation and Discussion

The contact space analysis procedure described above, as well as the fine-motion trajectory planner of [6], have been implemented on a Sun-4 workstation, in POPLOG (Pop-11 and Prolog) and *C*. CSG assembly part descriptions are parsed in Prolog, and the geometric solid modeller *ACIS* provides surface boundary descriptions of the parts, which serve to parameterize the primitive contact formulae in Appendices I and II. Computations of a combinatorial nature, such as the enumeration of 6–tuples of PCs performed to find the vertices of contact space, are executed in Pop-11. Numerically-intensive computations, such as the iterative refinement of vertex configurations described in section 3, are performed in *C*. Contact state adjacency graphs constructed through this technique are searched by the fine-motion planner [6] to generate reliable sequences of contact state transitions, together with command trajectories for traversing the selected states. Fine-motion plans thus generated for a square peg-in-hole assembly have been successfully executed by a Zebra-0 robot, with the aid of a visual servoing facility.

Since the calculation of a local contact space's vertices involves the enumeration of all 6–tuples of the PCs associated with the contact space, the computation time is proportional to

$$\binom{n}{6} = \frac{n!}{(n-6)!\,6!} \tag{8}$$

where n is the total number of PCs. As noted by Koutsou [13], it is useful to restrict the dimensions of contact space when enumerating its vertices, in order to limit the number of PCs and the resulting computation time. We have found it convenient to limit the rotational component of contact space by imposing positive tilts about the x, y, and z axes. For the square peg-in-hole contact space partially illustrated in figure 7, these constraints reduce the number of PCs from 32 to 9. The lack of constraining PCs produces a contact space

devoid of vertices, however, so three "virtual PCs" are added temporarily to the existing PCs to represent the imposed rotational limits $\delta x = -\epsilon$, $\delta y = -\epsilon$, and $\delta z = -\epsilon$, where $0 < \epsilon \ll 1$. Contact states involving virtual PCs are then filtered out of the resulting adjacency graph. For the square peg-in-hole assembly with $\frac{1}{32}$ inch clearances, the restricted contact space contains contact states of dimension $1, 2, 3, 4, 5$, numbering $2, 11, 24, 23, 9$, respectively.

The authors propose to merge their model-based fine-motion planning technique with the on-line compliance acquisition approach of Gullapalli [11][12]. Concerned primarily with the spatial aspects of fine-motion planning, our off-line planner's modelling of contact space topology complements the force-related capabilities of an on-line learning system, whose jamming-avoidance skills are difficult to replicate off-line. In the proposed fusion of methods, the fine-motion planner will produce a sequence of contact states in the contact space of an assembly, as well as a piecewise-linear command trajectory through the selected contact states. To accommodate the nonlinearities of contact space and avoid jamming in the presence of noise and uncertainty, the command trajectory will be augmented with a nonlinear compliant behavior, acquired on-line through associative reinforcement learning. The fine-motion planner's decomposition of contact space into topologically distinct facets will enable the learning system to devote separate neural networks to the different contact states, whose characteristic contact geometries call for qualitatively distinct compliances.

5 Conclusion

We have presented a method for analyzing local contact spaces for assemblies with narrow insertion clearances. The primitive contacts of a local contact space are characterized as bounded 5–dimensional surfaces, whose intersections in $\Re^6$ comprise the lower-dimensional facets of contact space. The vertices of contact space are calculated efficiently via the multivariable Newton method, and the topology of contact space is represented by an adjacency graph of contact states. The fine-motion planner described in the companion paper [6] searches this adjacency graph for a traversable sequence of contact state transitions, plotting a piecewise-linear trajectory in the selected states. Fine-motion plans thus generated for a square peg-in-hole assembly have been successfully executed by a Zebra-0 robot.

Appendix I

The primitive contact condition

$$(\mathbf{p} + \mathbf{dx} + RPY(\delta\mathbf{x})\mathbf{r}) \cdot \mathbf{n_c} = (\mathbf{p} + \mathbf{r} + \mathbf{dc}) \cdot \mathbf{n_c} \tag{9}$$

may be written

$$(\mathbf{dx} + RPY(\delta\mathbf{x})\mathbf{r}) \cdot \mathbf{n_c} - (\mathbf{r} + \mathbf{dc}) \cdot \mathbf{n_c} = 0 \tag{10}$$

Expanding $\mathbf{dx}$, δx, and $RPY(\delta\mathbf{x})$ as in section 2, we obtain the primitive contact function

$$\begin{aligned} f(\mathbf{X}) &= dx\,nx + dy\,ny + dz\,nz + \\ &\quad IB + JD + IE - JF + H n_z - \\ &\quad (\mathbf{r} + \mathbf{dc}) \cdot \mathbf{n} \\ &= 0 \end{aligned} \tag{11}$$

where

$$\begin{aligned} I &= C_y r_x + S_x S_y r_y + C_x S_y r_z \\ B &= C_z n_x \\ J &= S_x r_z - C_x R_y \\ D &= S_z n_x \\ E &= S_z n_y \\ F &= C_z n_y \\ H &= S_x C_y R_y + C_x C_y r_z - S_y r_x \end{aligned} \tag{12}$$

Appendix II

The outward normal **N** of a primitive contact C-surface is obtained by differentiating equation (11) with respect to the 6 components of the pose and then normalizing the resulting vector.

$$\nabla f = \begin{pmatrix} n_x \\ n_y \\ n_z \\ AB + CD + AE + CF + Gn_z \\ HB + HE - In_z \\ JB - ID + JE + IF \end{pmatrix} \tag{13}$$

and

$$\mathbf{N} = \frac{\nabla f}{|\nabla f|} \tag{14}$$

where

$$\begin{aligned} A &= C_x S_y r_y - S_x S_y r_z \\ C &= C_x r_z + S_x r_y \\ G &= C_x C_y r_y - S_x C_y r_z \end{aligned} \tag{15}$$

Taking $f_i(\mathbf{X})$ as PC_i's approximate distance to **X**, the surface tangent is approximated by the hyperplane

$$\mathbf{N}_i \cdot \mathbf{X} = D_i \tag{16}$$

where

$$D_i = \mathbf{X} \cdot \mathbf{N}_i - f_i(\mathbf{X}) \tag{17}$$

6 References

1. Ambler, A.P., Popplestone, R.J. (1975), "Inferring the positions of bodies from spatial relationships", *Artificial Intelligence*, Vol. 6, No. 2, pp. 157-174.
2. Buckley, C.E. (1985), "A proximity metric for continuum path planning", *9th International Joint Conference on Artificial Intelligence*, pp. 1096-1102.
3. Caine, M.E. (1985), "Chamferless assembly of rectangular parts in two and three dimensions", S.M. Thesis, Dept. of M.E., MIT.
4. Caine, M.E., Lozano-Pérez, T., Seering, W.P. (1989), "Assembly strategies for chamferless parts", *Proceedings of the IEEE International Conference on Robotics and Automation*, pp. 472-477.
5. Canny, J.F. (1989), "On computability of fine motion plans", *Proceedings of the IEEE International Conference on Robotics and Automation*, pp. 177-182.
6. Dakin, G., Popplestone, R.J. (1993), "Fine-motion planning in the contact space of narrow-clearance assemblies", (to appear) *Proceedings of the IASTED International Conference on Robotics and Manufacturing*, and Technical Report 93-60, C.S. Dept., Univ. of Massachusetts, Amherst MA.
7. Dakin, G., Popplestone, R.J. (1992), "Simplified Fine-Motion Planning in Generalized Contact Space", *Proc. of the IEEE International Symposium on Intelligent Control*, pp. 281-6.
8. Donald, B.R. (1984), "Motion planning with six degrees of freedom", Technical Report AI-TR-791, A.I. Laboratory, MIT.
9. Erdmann, M. (1984), "On motion planning with uncertainty", Tech. Report AI-TR-810, Artificial Intelligence Laboratory, MIT.
10. Gilbert, E.G., Johnson, D.W. (1985), "Distance functions and their application to robot path planning in the presence of obstacles", *IEEE Journal of Robotics and Automation*, Vol. RA-1, pp. 21-30.
11. Gullapalli, V. (1993), "Learning control under extreme uncertainty", in Giles, C.L., Hanson, S.J., Cowan, J.D. (eds), *Advances in Neural Information Processing Systems 5*, San Mateo CA: Morgan Kaufmann Publishers.
12. Gullapalli, V., Grupen, R.A., Barto, A.G. (1992), "Learning reactive admittance control", *Proceedings of the IEEE Conference on Robotics and Automation*, Vol. 2, pp. 1475-1480.
13. Koutsou, A. (1986), "Parts mating by moving objects in contact", PhD Thesis, Dept. of A.I., Edinburgh University.
14. Laugier, C. (1989), "Planning fine motion stategies by reasoning in contact space", *Proceedings of the IEEE International Conference on Robotics*

and Automation, pp.653-659.
15. Liu, Y. (1990), "Symmetry groups in robotic assembly planning", PhD Dissertation, COINS Dept., U.Mass., Amherst MA 01003.
16. Lozano-Pérez, T., Mason, M., Taylor, R.H. (1984), "Automatic synthesis of fine-motion strategies for robots", *International Journal of Robotics Research*, Vol. 3, No. 1, pp. 3-24.
17. Peshkin, M.A. (1990), "Programmed compliance for error corrective assembly", *IEEE Transactions on Robotics and Automation*, Vol 6, No. 4, pp. 473-482.
18. Popplestone, Ambler, A.P., Bellos, I. (1980), "An interpreter for a language describing assemblies", Artificial Intelligence, Vol. 14, No. 1, pp. 79-107.
19. Salisbury, J.K. (1980), "Active stiffness control of a manipulator in Cartesian coordinates", *Proceedings of the 19th IEEE Conference on Decision and Control*, pp. 95-100.
20. Whitney, D.E. (1985), "Historical perspective and state of the art in robot force control", *IEEE International Conference on Robotics and Automation*, pp. 262-268.